

## SUPPORTING INFORMATION

### V<sub>6</sub>O<sub>13</sub> films by control of the oxidation state from aqueous precursor to crystalline phase

Nick Peys<sup>a,b</sup>, Yun Ling<sup>c</sup>, Daan Dewulf<sup>a,d</sup>, Sven Gielis<sup>a,d</sup>, Christopher De Dobbelaere<sup>a</sup>, Daniel Cuypers<sup>b,e</sup>,  
Peter Adriaensens<sup>f</sup>, Sabine Van Doorslaer<sup>c</sup>, Stefan De Gendt<sup>b,e</sup>, An Hardy<sup>a,d</sup>,  
Marlies K. Van Bael<sup>a,d</sup>

<sup>a</sup>Hasselt University, Institute for Materials Research, Inorganic and Physical Chemistry, Diepenbeek, Belgium

<sup>b</sup>IMEC vzw, Heverlee, Belgium

<sup>c</sup>University of Antwerp, Department of Physics, SIBAC Laboratory, Antwerp, Belgium

<sup>d</sup>IMEC vzw, Division IMOMECE, Diepenbeek, Belgium

<sup>e</sup>KULeuven, Department of Chemistry, Heverlee, Belgium

<sup>f</sup>Hasselt University, Institute for Materials Research, Applied and Analytical Chemistry, Diepenbeek, Belgium

#### 1. FTIR on the dried citrato-oxovanadate(IV) precursor

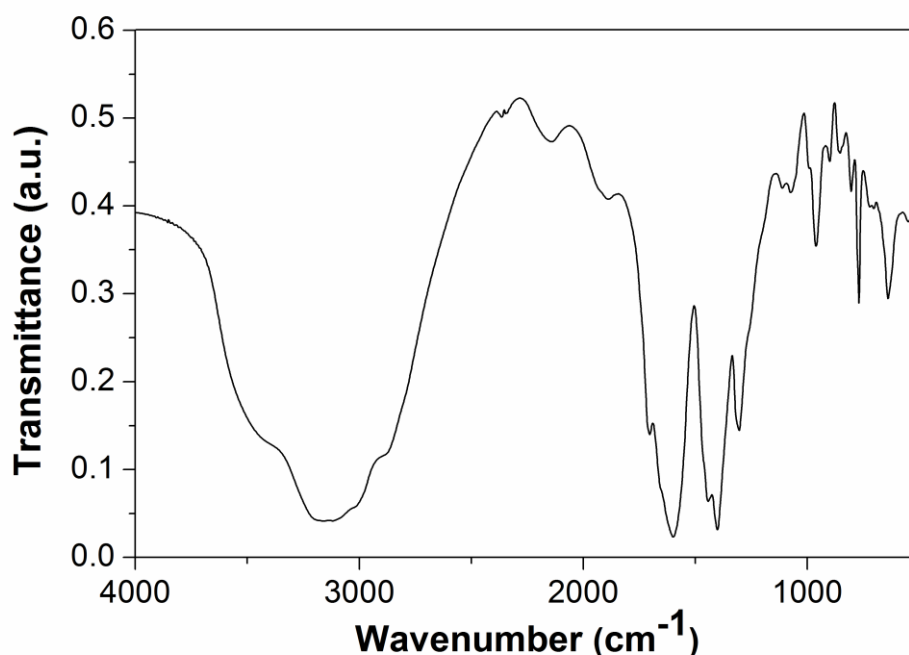


Figure S1: FTIR spectrum of the dried citrato-oxovanadate(IV) precursor:  $\nu_{as}(\text{C}=\text{O})$  in  $\text{COO}^-/\text{NH}_4^+$  at  $1703\text{ cm}^{-1}$ ,  $\nu_{as}(\text{C}=\text{O})$  in  $\text{COO}^-/\text{VO}_2^+$  at  $1590\text{ cm}^{-1}$ ,  $\nu_s(\text{C}=\text{O})$  in  $\text{COO}^-/\text{VO}_2^+$  at  $1400\text{ cm}^{-1}$  which coincides with the ammonium deformation  $\delta(\text{NH}_4^+)$ ,  $\nu(\text{C}-\text{OV})$  at  $1100\text{ cm}^{-1}$  and  $1070\text{ cm}^{-1}$ , and  $\nu(\text{V(IV)}=\text{O})$  in  $\text{VO}_2^+$  at  $976\text{ cm}^{-1}$ . The absorption bands between  $3700$  and  $2750\text{ cm}^{-1}$  are assigned to  $\nu(\text{O}-\text{H})$  as well as  $\nu(\text{N}-\text{H})$ , broadened by hydrogen bridges and  $\nu(\text{C}-\text{H})$ .<sup>1,2</sup>

## 2. CW-EPR spectra of samples A, B and C at room temperature

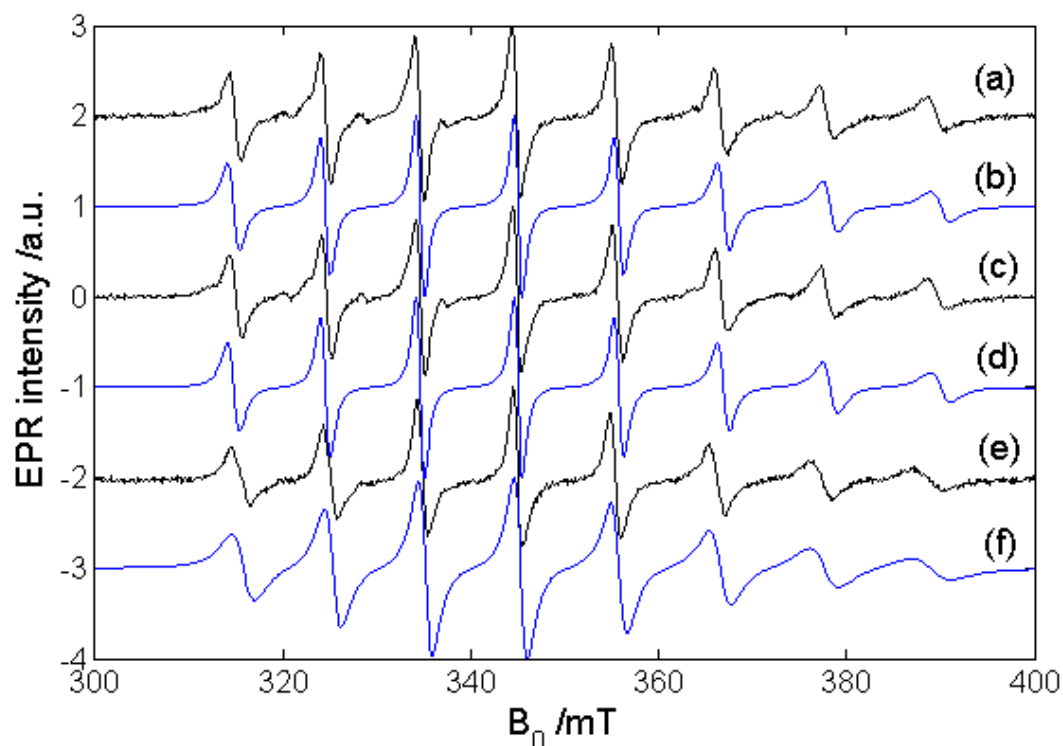


Figure S2. Experimental (black) and simulated (blue) room-temperature CW-EPR spectra of sample A (a,b), sample B (c,d) and sample C (e,f).

The room-temperature CW-EPR spectra of samples B and C could be simulated using the parameters reported in Table 2 (main text) and assuming a fast motion of the molecule with correlation times of  $4.10^{-11}$  s (sample B) and  $9.10^{-11}$  s (sample C), confirming that the isolated vanadyl species observed at low temperature persist at room temperature. No broad signal of vanadyl clusters was observed for these samples at room temperature, suggesting strongly that the broad feature found at low temperature is due to freezing-induced clustering. This is corroborated by the fact that the room-temperature CW-EPR spectrum of sample A is identical of that of sample B. This not only indicates that the same isolated vanadyl ligation modes are present in both samples, it also shows that the dominant broad signal found for sample A at low temperature is most likely due to freezing-induced clusters.<sup>1</sup> Apparently the presence of citric acid induces better glass formation at low temperature (and hence less freezing-induced clustering of the vanadyl complexes).

<sup>1</sup> Note, that the clustered species may be unobservable at room temperature due to relaxation issues.

### 3. Simulation of the CW-EPR spectra at 100 K

In the following, the CW-EPR spectra of samples B, C, D are simulated using the parameters given in Table 2 of the main text.

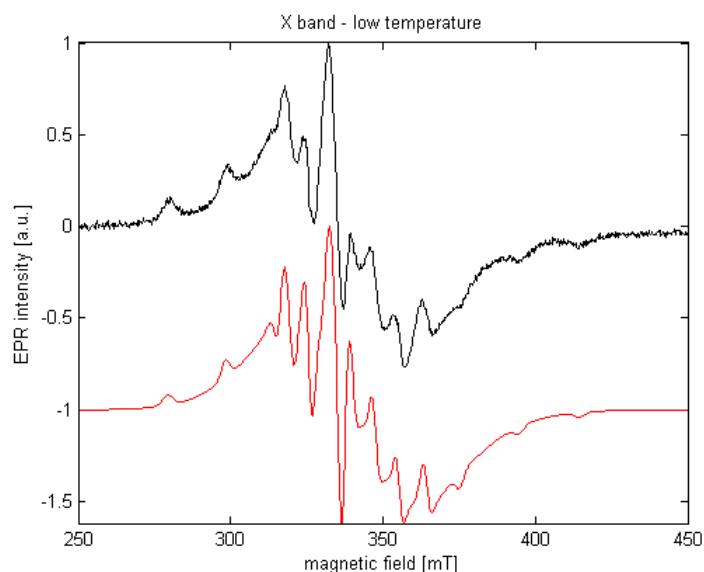


*Figure S3. Experimental (black) and simulated (red) EPR spectrum of sample B. The simulated spectrum is the sum of a spectrum due to the mononuclear species (parameters from Table 2 in main text) and a broad feature around  $g=1.99$  mimicking the dipolarly interacting oxovanadate(IV) centers (clusters).*

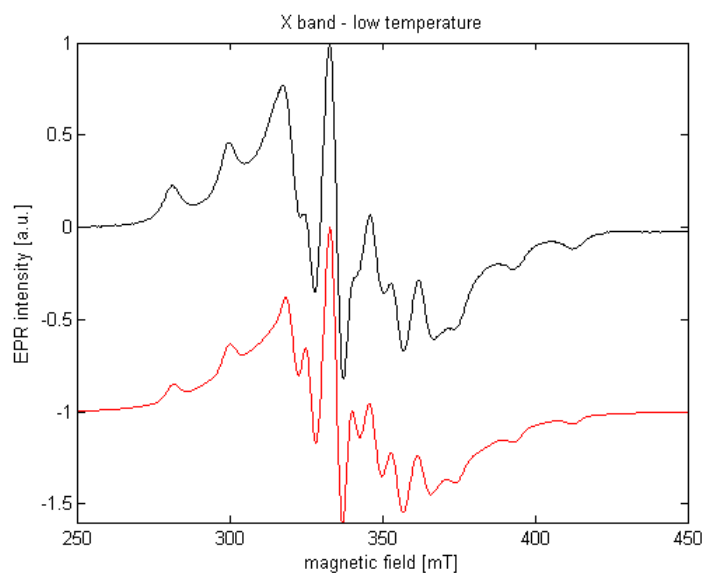


*Figure S4. Experimental (black) and simulated (red) EPR spectrum of sample C. The simulated spectrum is the sum of a spectrum due to the mononuclear species (parameters from Table 2 in main text) and a broad feature around  $g=1.99$  mimicking the dipolarly interacting oxovanadate(IV) centers (clusters).*

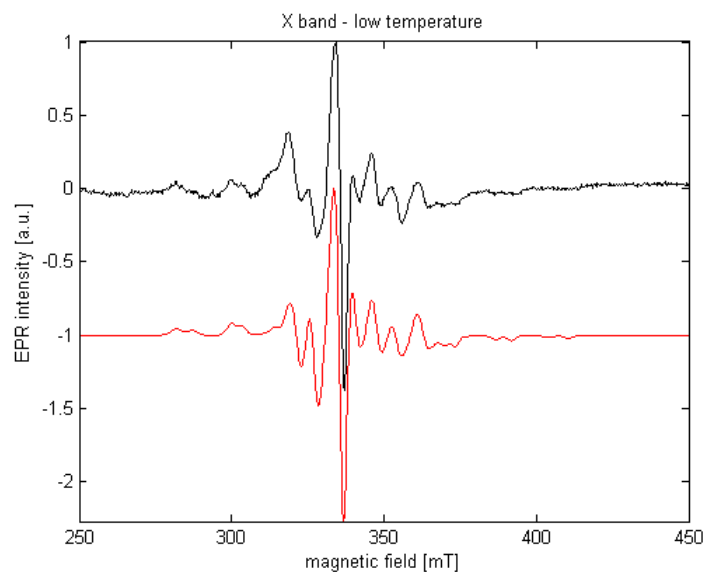


Figure S5. Experimental (black) and simulated (red) EPR spectrum of sample D. The simulated spectrum is the sum of two contributions due to mononuclear species (parameters from Table 2 in main text).

#### 4. HYSCORE spectra

In the following, the HYSCORE spectra taken at  $B_0=348$  mT are shown for sample D. This is an observer position at which all molecular orientations are contributing. In the HYSCORE spectra, only a small feature around the proton Larmor frequency ( $\sim 15$  MHz) is observed with maximal width of 2.5 MHz. No contributions of  $^{14}\text{N}$ -related cross peaks can be observed, excluding equatorial ligation of the ammonia.

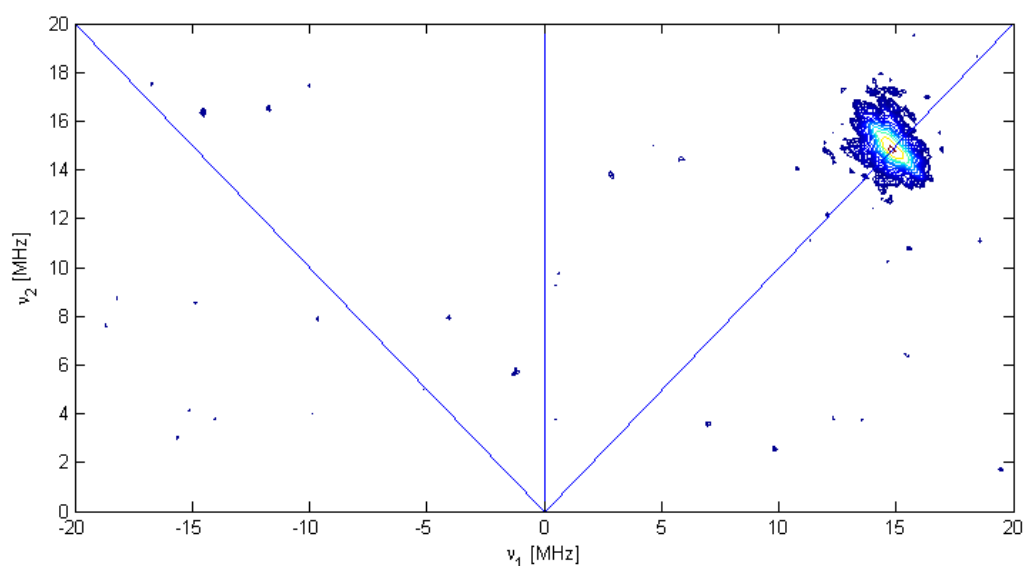


Figure S6. Experimental HYSCORE spectrum of sample D taken at observer position  $B_0=348$  mT. All further experimental details can be found in the main text.

5. GATR-FTIR spectra of single layered spin coated films followed by an intermediate anneal in N<sub>2</sub> or 0.1 % O<sub>2</sub> (400 °C, 10 minutes).

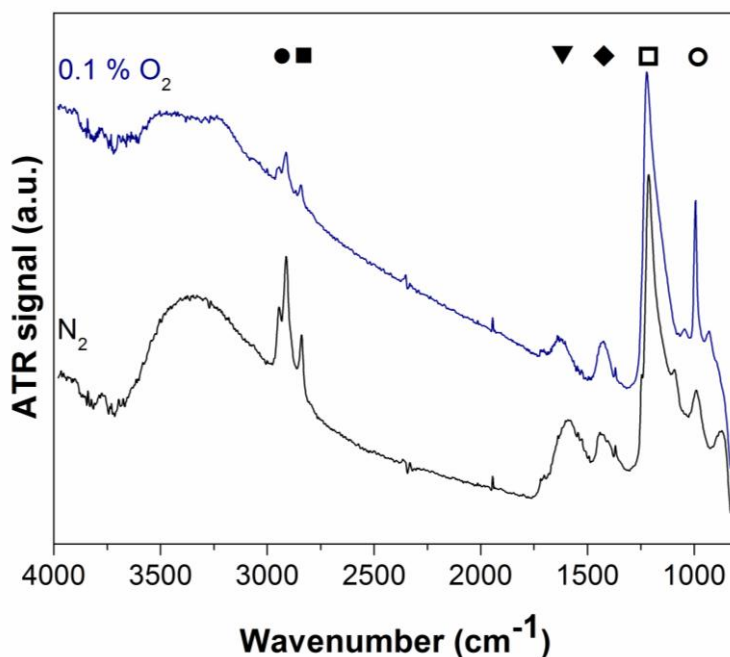


Figure S7: GATR-FTIR spectra with possible IR assignments of a single spin coated layer on 1.2 nm SiO<sub>2</sub>, followed by an intermediate anneal in N<sub>2</sub> or in 0.1 % O<sub>2</sub> (400 °C, 10 minutes): ●  $\nu_{as}(\text{C-H})$  in CH<sub>2</sub>, ■  $\nu_s(\text{C-H})$  in CH<sub>2</sub>, ▼  $\nu_{as}(\text{C=O})$  in COO<sup>-</sup>/VO<sup>2+</sup>, ◆  $\nu_s(\text{C=O})$  in COO<sup>-</sup>/VO<sup>2+</sup>, □ SiO<sub>2</sub> LO mode<sup>3</sup>, ○  $\nu(\text{V(IV)=O})$  in VO<sup>2+</sup>.

6. Reference

1. C. Djordjevic, M. Lee and E. Sinn, *Inorganic Chemistry*, 1989, **28**, 719-723.
2. K. Nakamoto, *Infrared and Raman Spectra of Inorganic and Coordination Compounds. Part B: Applications in Coordination, Organometallic, and Bioinorganic Chemistry*, 5 edn., Wiley & Sons, New York, 1997.
3. K. Ishikawa, Y. Uchiyama, H. Ogawa and S. Fujimura, *Applied Surface Science*, 1997, **117–118**, 212-215.